Materials Today Communications 26 (2021) 102134

Contents lists available at ScienceDirect

Materials Today Communications

journal homepage: www.elsevier.com/locate/mtcomm

Controlled drug release from electrospun PCL non-woven scaffolds via multi-layering and e-beam treatment

Apollinariya A. Volokhova [a,c], Valeriya L. Kudryavtseva [a,d], Tatiana I. Spiridonova [a], Ilya Kolesnik [a], Semen I. Goreninskii [b], Roman V. Sazonov [e], Gennady E. Remnev [e], Sergei I. Tverdokhlebov [a,*]

[a] National Research Tomsk Polytechnic University, B.P. Veinberg Research and Educational Center, 30 Lenin Avenue, Tomsk, 634050, Russian Federation
[b] National Research Tomsk Polytechnic University, N.M. Kizhner Research and Educational Center, 30 Lenin Avenue, Tomsk, 634050, Russian Federation
[c] National Research Tomsk State University, 36 Lenin Avenue Tomsk, 634050, Russian Federation
[d] Queen Mary University of London, Mile End Rd, Bethnal Green, London, E1 4NS, United Kingdom
[e] National Research Tomsk Polytechnic University, Research and Production Laboratory "Pulse-Beam, Electric Discharge and Plasma Technologies", 30 Lenin Avenue, Tomsk, 634050, Russian Federation

ARTICLE INFO

Keywords:
Drug delivery devices
Electron beam treatment
Biodegradable materials
Polycaprolactone
Electrospinning

ABSTRACT

Currently, electrospun synthetic bioresorbable polymer scaffolds are applied in regenerative medicine and tissue engineering as targeted drug delivery devices because of their mechanical and physico-chemical properties. To control the rate of polymer degradation and drug release from polymer scaffolds, surface modification techniques are widely used. In this study, paracetamol-loaded poly (ε-caprolactone) electrospun fibrous scaffolds were treated by the pulsed electron beam irradiation. Pure control PCL scaffold, as well as scaffolds with four paracetamol concentrations (2 wt./wt. %, 8 wt./wt. %, 16 wt./wt. %, and 32 wt./wt.%) were modified. The mechanical and chemical properties and morphology of modified materials were examined. The sustained release of the model drug over a period of one hour for both non-treated and treated samples was demonstrated. It was shown that treatment leads to an increase in drug release rate and does not change surface morphology of scaffolds and fibers diameter distribution.

1. Introduction

The present-day medicine requires targeted delivery and controlled release of drugs [1]. Drug delivery systems are intended to deliver well-controlled amounts of drug between the minimum effective level and the toxic level within a predetermined time interval [2–4]. Drug carriers must be in direct contact with the tissues and organs of the human body, which determines the requirements for their properties [5,6]. One of the currently relevant types of carriers are scaffolds obtained by the electrospinning method [7]. There are many studies where the latter are presented as drug delivery agents [8,9].

Their advantages include biocompatibility, elasticity, manufacturability of the production process, and high reproducibility of methods [10,11]. However, there are also disadvantages, the presence of the burst release effect being the most important in this context.

Burst release is a high and very fast initial drug delivery [12]. Control of burst release effect is essential either to avoid toxicity or to ensure immediate action at the targeted location as in the case of antibiotics [13] and cytostatics [14].

The articles describe various factors affecting drug release from fibers and causing burst release [15]: polymer molecular weight, matrix wettability and swelling ability, fiber and drug crystallinity, polymer-drug interaction, thickness scaffold, etc.

To simplify the description of the burst release effect and the kinetic release curves in general, we introduce two parameters: TTP (time to plateau) and QTP (quantity to plateau). The first parameter reflects the time needed for the release schedule to reach a plateau, that is, for the drug to stop arriving into the considered area/environment. The second parameter reflects the total amount of drug released during the plateau reached. Considering the parameters entered, burst release is a process characterized by low TTP values.

However, low QTP values are also a problem because QTP largely determines the effectiveness of targeted delivery and controlled release. If the drug leaves the fiber and is washed from its surface too quickly,

* Corresponding author.
E-mail address: tverd@tpu.ru (S.I. Tverdokhlebov).

https://doi.org/10.1016/j.mtcomm.2021.102134
Received 22 October 2020; Received in revised form 3 February 2021; Accepted 5 February 2021
Available online 12 February 2021

then it is reasonable to create a diffusion barrier that would inhibit this process. This approach considers a formation of pure polymer fibrous layer formation on the surface of drug-loaded layers. In [16] "barrier meshes" were used as a regulatory layer for the retarded release of the secondary drug and as a result a time-programmed dual-drug sustained release system was obtained. Multilayer scaffolds' fabrication technique used in this study was previously designated as sequential electrospinning [17]. Applying the technological advantages of electrospinning and the multilayering methodology, a formulation that controls the release behavior of incorporated drug is anticipated.

Because diffusion is not the sole factor affecting the release, others can be varied to achieve this goal. In particular, there are surface modification methods that change the surface properties of scaffolds and affect drug release [18,19].

Several physico-chemical modification methods have been proposed to control the rate of degradation and drug release from polymer scaffolds [20,21]. One of the advanced methods is the pulsed electron beam treatment, which was shown to increase hydrophilic properties [22] and degradation rate through decreasing the average molecular weight of the bulk polymer and pseudo-surface erosion [23–27]. This method allows obtaining required properties of the polymer by excitation and ionization of its molecules. Radiolysis is accompanied by an extensive formation of ions and excited neutral particles (radicals) with high chemical activity. These particles react with each other, molecules, and with atoms of the system under irradiation. Thus, electron beam irradiation allows cross-linking or scissoring of polymer molecules depending on the particle's energy and absorbed dose [28,29]. Previously it was shown that electron beam irradiation could be an effective tool to modify bioresorbable polymeric material in order to change their crystallinity and degradation rate [26].

E-beam could lead to decomposition of the drug. However, when the drug is in solid state, most of the systems show a lower loss of activity after ionizing irradiation [30]. The resistance was showed for several drugs such as doxorubicin hydrochloride [31], norfloxacin and gatifloxacin [32], and many other [33].

Therefore, such changes as pseudo-surface erosion, etching, formation of reactive sites, chain scission, or cross-linking in polymer structure will lead to changes in release profile of loaded substances without loss of activity of the drug.

In this paper, we propose to study, both individually and in combination, the effect of the barrier layers addition and treatment with a pulsed electron beam on scaffolds properties, and to evaluate the possibility of their application to regulate drug release from scaffolds.

In this study we have chosen scaffolds based on polycaprolactone [34]. Poly(ε-caprolactone) (PCL) is semicrystalline, biocompatible, and bioresorbable polymer that has US Food and Drug Administration approval for several biomedical devices [35]. PCL is suitable material for both long-term drug delivery, for example, in birth control implants [36] and short-term release of antibiotics [37,38], anti-inflammatory agents [39], bone morphogenetic proteins [40], immune modulators [41], and naturally occurring biologically active compounds [42]. The increased interest in scaffolds based on polycaprolactone is caused by good mechanical properties of the material at its affordable price. However, the main disadvantage of this material as a drug delivery agent is its hydrophobicity, burst release effect, and slow degradation rate in the body, which leads to a weak drug desorption and diffusion process [34].

Paracetamol was chosen as a model drug because it is a research-convenient representative of the low-molecular-weight drugs poorly soluble in water [43]. Local release is useful for poorly soluble drugs administration because of the need to reduce systemic doses [44].

Aim of this study is to investigate the effects of electron-beam irradiation on the kinetics of poorly water-soluble drug release from poly (ε-caprolactone) electrospun monolayer and composite multilayer scaffolds and assess its potential for creating an integrated approach to controlled drug release systems.

2. Materials and methods

2.1. Materials

PCL (Mw = 80,000) was purchased from Sigma–Aldrich (St. Louis, MO), Hexafluoroisopropanol (HFIP) (Ekos-1, Russia) was used as a solvent for preparation of the spinning solutions. Monoclinic paracetamol powder (USP grade, form I) was purchased from Shandong Xinhua Pharmaceutical (China). Phosphate Buffer Saline (PBS, pH 7.4) used for drug release modelling was purchased from Biolot (Russia).

2.2. Preparation of PCL fibers by electrospinning

The polymer solution with concentration of 7 wt.% was prepared by dissolving PCL and paracetamol with a weight ratio of 2, 8, 16, and 32 wt./wt.% in HFIP and left for 24 h at room temperature. Before electrospinning, the solutions were stirred for 20 min at room temperature until total homogenization. The solution was electrospun (NANON-01A, MECC CO., LTD., Japan) from 8 mL syringe with a 0.5 mm needle (G21) and a 5 mL/h flow rate. A high voltage (20 kV) was applied to the tip of the needle attached to the syringe when a fluid jet was ejected. The resulting fibers were collected on 200 mm diameter drum collectors with 50 rpm set rotation speed and 130 mm syringe-collector distance.

Two groups of paracetamol-loaded PCL scaffolds were obtained, namely, monolayer materials and composite scaffolds with pure PCL fiber barrier layers on the both sides of drug-loaded scaffold. All groups of experimental samples are schematically depicted in Fig. 1.

Composite scaffolds were produced as follows: firstly, 8 mL of 7 wt.% of pure PCL in HFIP was electrospun onto the collector, then the syringe was replaced with the one with 2, 8, 16, and 32 wt./wt.% paracetamol/PCL solution (8 mL). The chosen solution was electrospun on the surface of already collected pure PCL fibers. Following that, the third syringe with pure PCL solution was electrospun forming a barrier layer for further drug release identical with the initial layer of PCL fibers.

Average thickness of each scaffold was determined by distance measurement of both free scaffold surfaces (TN-60, KRIM, Russia). Specimens were placed between two metal stamps, and distance was indicated by a rangefinder. Because of the soft tissue composition, especially of the acellular implants, the approximation of the rangefinder-stamps was connected with a pressure gauge to indicate the point of approximation, where the matrix scaffold was compressed.

After electrospinning, scaffolds were removed and placed into a custom-made vacuum camera for 24 h (7×10^{-3} Pa) to remove residual solvents.

2.3. Pulsed electron beam irradiation

Electron beam irradiation of PCL scaffolds was conducted using pulsed e-beam accelerator TEA-500 [45] within 25 kGy of absorbed dose in the air under atmospheric pressure. The electron beam diameter was 5 cm, beam kinetic energy beam was 350−400 keV, current varied between 6–9 kA, duration of 1 pulse at half-maximum was 60 ns, and the electron beam energy equaled 90 J. The thickness of the titanium foil in the accelerator exit window equaled 50 μm.

Schematic representation illustrating the functional diagram of accelerator and sample arrangement during irradiation is presented in Fig. 2.

2.4. Scanning electron microscopy (SEM)

SEM images were used to determine the diameter distributions of the nanofibers. Samples of each polymer scaffold were fixed onto metallic studs with a double-sided conductive tape. A thin gold film was sprayed onto samples to provide a contact of the material with the stub and to prevent the accumulation of a negative charge on the samples' surface.

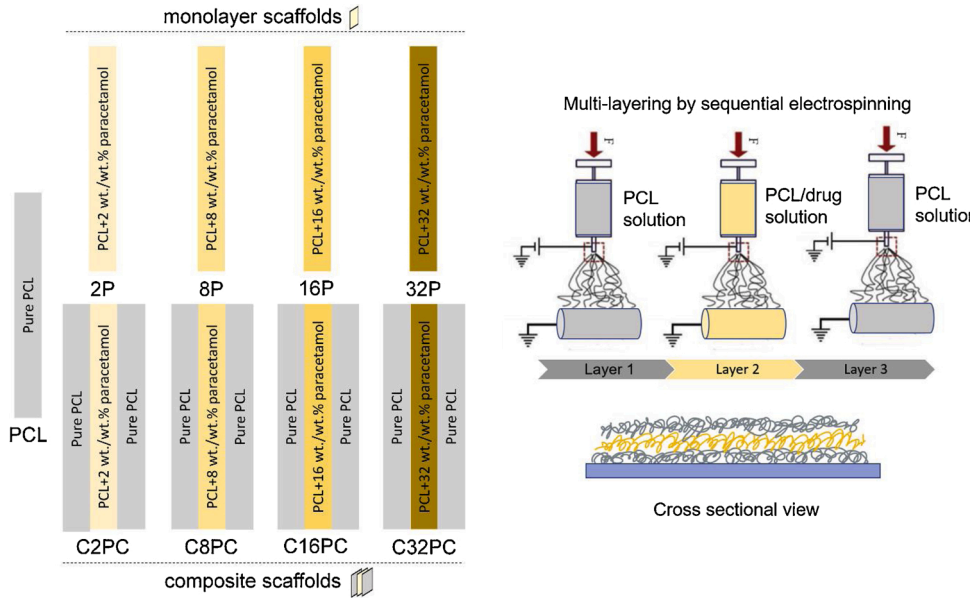

Fig. 1. Groups of paracetamol-loaded samples obtained. PCL – pure PCL, 2 P (8 P, 16 P, 32 P) – paracetamol loaded fibers with 2 (8,16,32) wt./wt.% loading respectfully; C2(8,16,32) PC – composite scaffolds with barrier layers of pure PCL fibers on the both sides of drug-loaded scaffolds.

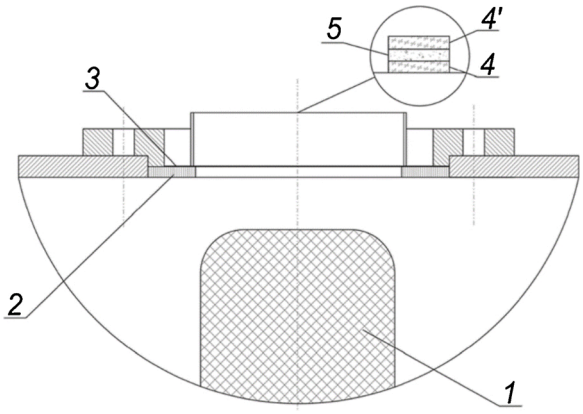

Fig. 2. Exit window of the electron accelerator: *1* – cathode; *2* – supporting grid; *3* –anode; *4*, *4′* – radiation monitoring films; *5* – sample [46].

The morphology of the sample was observed with a scanning electron microscope VEGA3 TESCAN (Tescan Analytics, France). One hundred randomly selected nanofibers were measured using ImageJ 1.44p software (National Institutes of Health, Bethesda, MD, USA) to calculate the diameter distributions of the nanofibers.

2.5. Fourier-transform infrared spectroscopy

IR spectra of the fabricated scaffolds were recorded within 650 to 4000 cm^{-1} using Cary 630 spectrometer (Agilent, USA). The obtained spectra were treated using Origin.Pro 8.1 software (OriginLab, USA).

2.6. Gel permeation chromatography (GPC)

GPC was used to determine the relative molecular weight of polymer in the samples of obtained scaffolds. The samples were dissolved in chloroform to 1.000 g/l and analyzed on Agilent 1200 LC system with refractive detector (Agilent technologies, USA). Flow rate was 1 mL/min; injection volume was 50 μL. Average molecular weight (Mw) was chosen as a reference point.

2.7. Thermogravimetric analysis (TGA)

Thermogravimetric analysis (TGA) was used to determine the mass loss curves of samples and to analyze their thermal behavior. The studies were performed using differential scanning calorimeter DSC Q2000 (TA Instruments, USA) in a dry air atmosphere using a heating rate of 10 °C/min and a temperature range of 25 °C–550 °C.

2.8. X-ray diffraction (XRD)

Crystal structure of the materials obtained was studied by means of X-ray diffraction method using Shimadzu XRD 6000 diffractometer (Shimadzu Corporation, Japan). The analysis was performed within 7−35° with the step size of 0.02° and the signal collection time at 2 s. CuK_α radiation with the wavelength of 1.54056 Å and accelerating voltage of 40 kV were applied.

The Scherrer equation was employed to calculate the crystallite sizes from the full-width at the half maximum (FWHM) of the PCL main peaks ($2\theta = 23°$ and $2\theta = 21°$) [47]:

$$L_{hkl} = \frac{K\lambda}{\beta\cos\theta}, \quad (1)$$

where L_{hkl} is size of the ordered (crystalline) domains; β – FWHM, the width of profile at the 1/2 position (half-peak width) of the maximum intensity from the background; θ is the scattering angle; λ is the X-ray wavelength; K is constant (here K=0.94).

Degree of crystallinity was calculated as a percentage of the scattered intensity of the crystalline phase over the scattered intensity of the crystalline and amorphous phase:

$$\chi = \frac{\sum_{i=1}^{n} S^i_{cryst}}{S_{amorph} + \sum_{i=1}^{n} S^i_{cryst}}, \quad (2)$$

where S^i_{cryst} – crystalline peak area; S_{amorph} – crystalline halo area.

The diffraction patterns were visualized using Origin.Pro 8.1 software (OriginLab, USA). Degree of crystallinity and crystallite sizes were calculated using special Crystal Impact Match! (Crystal Impact Co, Germany) software.

2.9. Wettability

The scaffolds wettability was characterized by depositing 30 μL drops of polar liquid (water and glycerin) at different positions on the samples in a Krüss EasyDrop contact-angle measurement system (Germany) and capturing the images one minute after depositing the drops. All data are represented as the averages and standard deviations of the measurements taken at four different spots on the surface of the respective sample. The total surface energy, its polar and dispersion components were calculated with the Owens-Wendt method.

2.10. Drug release study

Untreated and e-beam treated electrospun PCL scaffolds of 10 × 10 mm area, both with the incorporated drug, were immersed in Phosphate Buffer Saline (PBS, pH 7.4) at 25 °C for 24 h with four replicates for each type of scaffold. The experiments were run in 2 mL of PBS without stirring, and the drug release results were found to be within one standard deviation to each other. At predetermined time points, a 1 mL aliquot was withdrawn for further analysis and replaced with an identical volume of the fresh medium. The amount of released paracetamol was determined using UV–vis spectrometry (Shimadzu UV-1280, Shimadzu Corporation, Japan), detection wavelength – λ =245 nm. Concentration in the corresponding withdrawn aliquot was calculated from the calibration curve approximated by linear equation.

2.11. Mechanical testing

Tensile properties were measured at ambient temperature using an Instron 3369 testing machine (Illinois Tool Works, USA) equipped with a 50 N load cell. 60 × 20 mm test pieces were cut from the scaffold mats. A cross-head speed of 10 mm·min^{-1} was used. Strain was measured from cross-head separation and referred to 10 mm initial length. A minimum of 5 samples were tested for each material. Experimental data were analyzed with Bluehill® Universal software.

3. Results and discussion

3.1. Morphology study

All prepared polymer solutions exhibited sufficient spinnability forming defect-free scaffold mats with high repeatability. Results of scaffolds' thickness assessment are presented in Table 1.

It is known that thickness affects not only scaffolds *in vivo* behavior [48] but also drug release process [16], therefore, it is important to remark that increase in drug loading and further e-beam irradiation do not significantly affect this parameter for both monolayer and composite materials. Composite scaffolds were characterized with higher thickness value because of simple superposition of all three layers thicknesses.

To investigate the effect of e-beam irradiation and drug loading on the morphology of paracetamol-loaded PCL scaffolds, SEM was carried out. The SEM images of all groups of monolayer samples, as well as fiber diameter distributions, are shown in Fig. 3. The surface of composite materials with barrier layers is similar to the surface of the control sample. A statistical analysis was carried out in order to evaluate the change in the fiber diameters after the e-beam treatment.

Drug loading and e-beam irradiation do not significantly change the mean fiber diameters (Table 2). This information contributes well to the further study because it was shown that fiber diameter affects drug release rate [15,49]. Moreover, the fiber diameter and its uniformness is crucial parameter for cellular attachment modulating and proliferation [50].

Fibers' surface for all samples except 32 P (Fig. 3 J) is smooth with no defects, breakages, or diameter fluctuation. There are visible crystals on the 32 P sample surface (Fig. 3 J, red arrow), which can be contributed to paracetamol crystals. This indicates that at high concentrations, part of the drug is distributed over the surface of the fibers and can crystallize during the solvent evaporation in the electrospinning process. The effect of uneven volume distribution is described in [12], where the trapped drug can be released immediately from the surface of the polymer, especially in the case of high drug concentration.

According to previous studies, the reason for paracetamol surface distribution may be the initial crystallinity of incorporated drug powder [51,52]. This fact may affect drug release from scaffolds: at high concentrations a drug is mainly deposited on the surface in direct contact with liquid, which often results in burst release profile [53].

Table 1
Thickness of non-irradiated and irradiated PCL samples mats (For interpretation of the references to colour in this figure legend, the reader is referred to the web version of this article.).

	Sample thickness, μm	
	Before e-beam treatment	After e-beam treatment
PCL	128 ± 20	128 ± 21
2 P	110 ± 20	112 ± 20
8 P	118 ± 30	117 ± 18
16 P	112 ± 24	112 ± 20
32 P	118 ± 28	120 ± 19
C2 PC	450 ± 15	450 ± 20
C8 PC	450 ± 17	451 ± 21
C16 PC	432 ± 15	445 ± 25
C32 PC	443 ± 16	450 ± 23

3.2. Fourier transform infrared (FT-IR) spectroscopy

In order to assess whether drug incorporation and further treatment affected the chemistry of PCL and drug molecules, we performed FTIR spectroscopy.

With the increase of paracetamol concentration, its adsorption bands appeared on IR spectra of the fabricated materials (Table 3, Fig. 4) [54]. It can be effectively observed on the 32 P sample spectra. Moreover, the bands correspond to the monoclinic form of paracetamol, which correlates with the further XRD data.

With that, characteristic adsorption band of PCL (1721 cm^{-1}, C═O stretching vibrations) did not change its position [55]. Thus, it may be suggested that there were no intermolecular interactions between PCL and paracetamol.

At the same time, the observed adsorption bands corresponding to PCL and paracetamol were observed on the FTIR spectra of the materials treated with e-beam. It may be suggested that the chemical structures of both the polymer and drug did not change significantly during the treatment and the drug does not undergo phase transitions.

3.3. Gel permeation chromatography (GPC)

It was previously shown that electron beam treatment can significantly affect molecular weight of polymer towards both its increase or decrease [21,56,57]. The polymer degradation after irradiation process may be detected by the reduction of molecular weight of irradiated materials. The change in molecular weight of PCL scaffolds with different paracetamol content before and after pulsed e-beam irradiation was studied using gel permeation chromatography (GPC). The results are presented in Table 4.

With the increase in the drug concentration in the spinning solution, the molecular weight of the resulting fiber material does not change. After exposure to a pulsed electron beam irradiation, the molecular weight of the samples tends to decrease. Previously it was shown that the electron beam irradiation of PCL results in both crosslinking and chain scission process, without a predominance of one mechanism over the other [20]. Low molecular weight compounds, oligomers short macromolecules may form in considerable amount in an irradiated material, while at the same time, longer branched macromolecules are

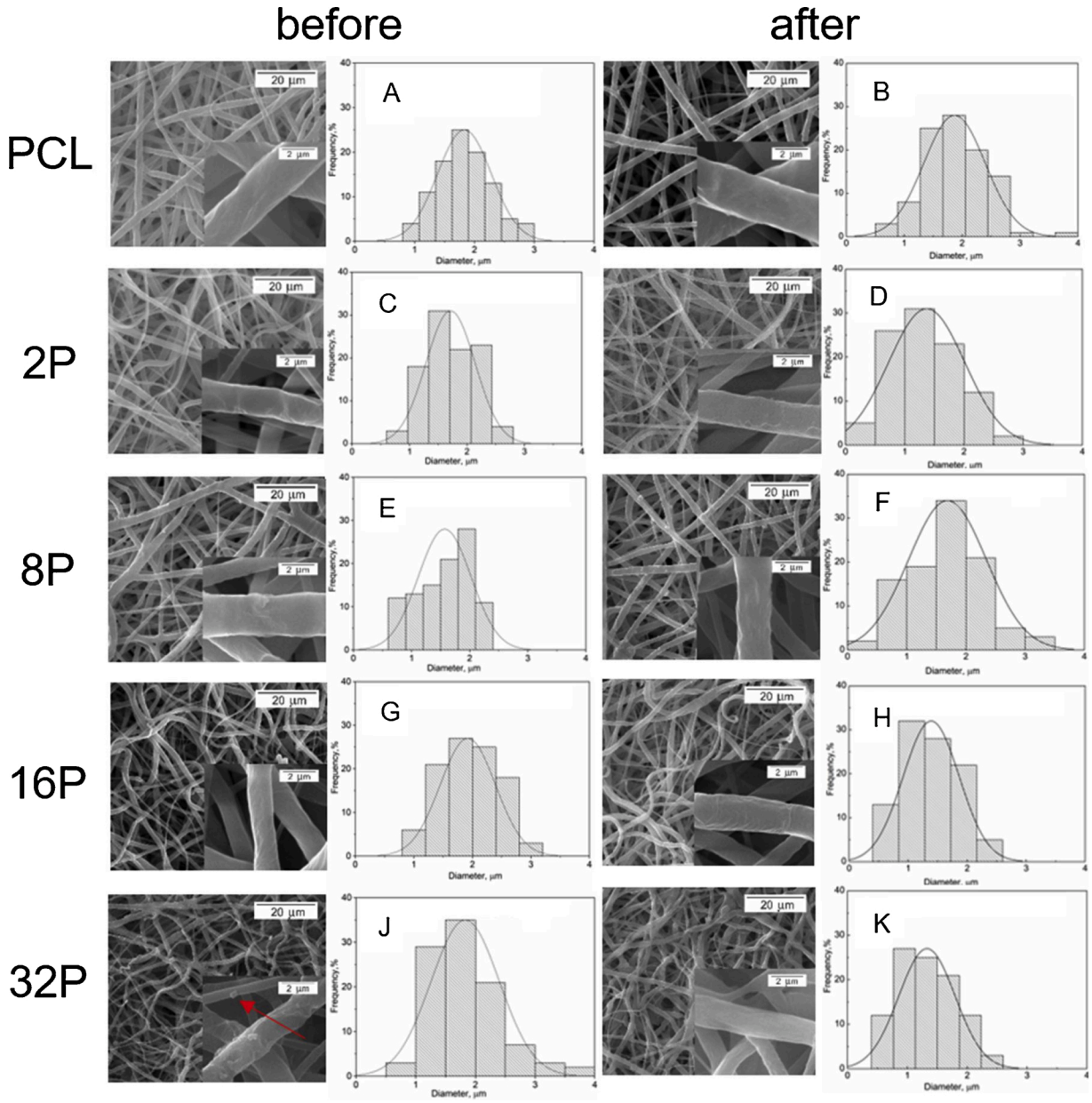

Fig. 3. SEM images of untreated and e-beam treated control pure electrospun PCL scaffold (A, B), PCL nanofibers loaded with 2 wt./wt.% (C, D), 8 wt./wt.% (E, F), 16 wt./wt.% (G, H), 32 wt./wt.% (J, K) paracetamol, respectively.

Table 2
Mean fiber diameter of non-irradiated and irradiated PCL samples.

	Mean fiber diameter, nm				
Sample	PCL	2p	8p	16p	32p
Before e-beam treatment	1.83 ± 0.45	1.71 ± 0.43	1.57 ± 0.45	1.92 ± 0.47	1.83 ± 0.57
After e-beam treatment	1.87 ± 0.53	1.37 ± 0.64	1.69 ± 0.66	1.39 ± 0.47	1.33 ± 0.47

created. The higher doses the irradiation leading to more pronounced effect, where an increase in the molecular weight might dominate over the processes of polymer degradation [58]. Revealing such a pattern is important, since it is known that the drug is released faster from fibers based on polymers with a lower molecular weight [59,60].

3.4. Thermogravimetric (TG) analysis

The interaction of components in multicomponent materials is frequently reflected in their thermal behavior [61]. Therefore, TGA analysis was performed in order to assess the possibility of nonspecific interactions between the drug and the polymer carrier.

Thermal properties of pure PCL and PCL/paracetamol scaffolds were performed by TG analysis (Fig. 5). In general, PCL shows single stage thermal degradation [62]. The PCL decomposed completely in the region of 270 °C–420 °C. PCL/paracetamol scaffolds (2 P and 8 P) also showed a single stage thermal degradation. 16 P and 32 P scaffolds decomposition was recorded in two stages. In the first stage, weight loss

Table 3
Observed adsorption bands of paracetamol [54].

Adsorption band, cm^{-1}	Corresponding vibration
1371	δ (CH_3)
1442	δ (CH_3), ν (Ph)
1506	δ (CNH), ν (Ph)
1565	δ (CNH), ν (Ph)
1610	ν (Ph)
1653	ν (C = O), δ (CNH)

from 170 °C to 300 °C may be attributed to paracetamol decomposition [55,63], while the second stage starting at around 300 °C and completing at around 420 °C, is the main thermal degradation zone and it corresponds to a polymer matrix degradation.

The e-beam treatment does not significantly affect pure PCL and 2 P, 8 P samples profiles but changes 16 P profile from two stages to one stage decomposition (Fig. 5 B). Thermal behavior of all studied samples is depicted in Table 5. T_{max} which corresponds to the maximum degradation rate also does not change significantly in the result of the e-beam treatment. 32 P exhibits two peaks at 278 °C and 395 °C of T_{max}; 16 P

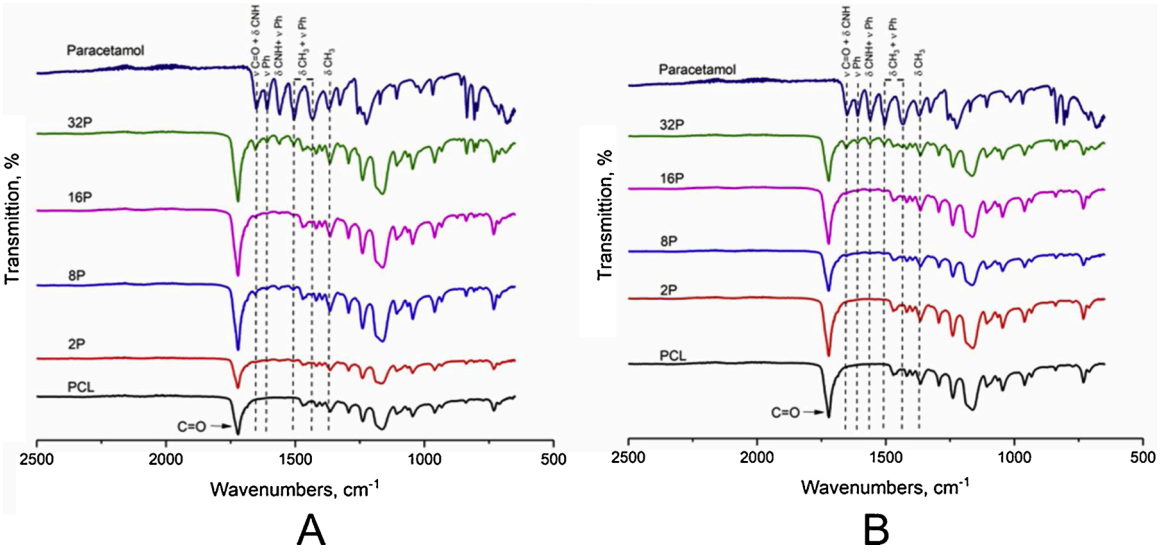

Fig. 4. FTIR-spectra of untreated (A) and e-beam treated (B) monolayer electrospun pure PCL scaffolds (black line), 2 wt./wt.% paracetamol loaded (red line), 8 wt./wt.% (blue line), 16 wt./wt.% (pink line), 32 wt./wt.% (green line) paracetamol respectively. Deep blue line represents FTIR-spectra of paracetamol powder (For interpretation of the references to colour in this figure legend, the reader is referred to the web version of this article.).

Table 4
Molecular weight of non-irradiated and irradiated PCL samples.

	$M_W \cdot 10^5$, g/mol				
Sample	PCL	2 P	8 P	16 P	32 P
Before e-beam irradiation	2.73 ± 0.21	2.36 ± 0.28	2.31 ± 0.16	2.52 ± 0.56	2.81 ± 0.39
After e-beam irradiation	2.08 ± 0.18	1.7 ± 0.76	2.33 ± 0.10	1.82 ± 0.07	2.17 ± 0.19

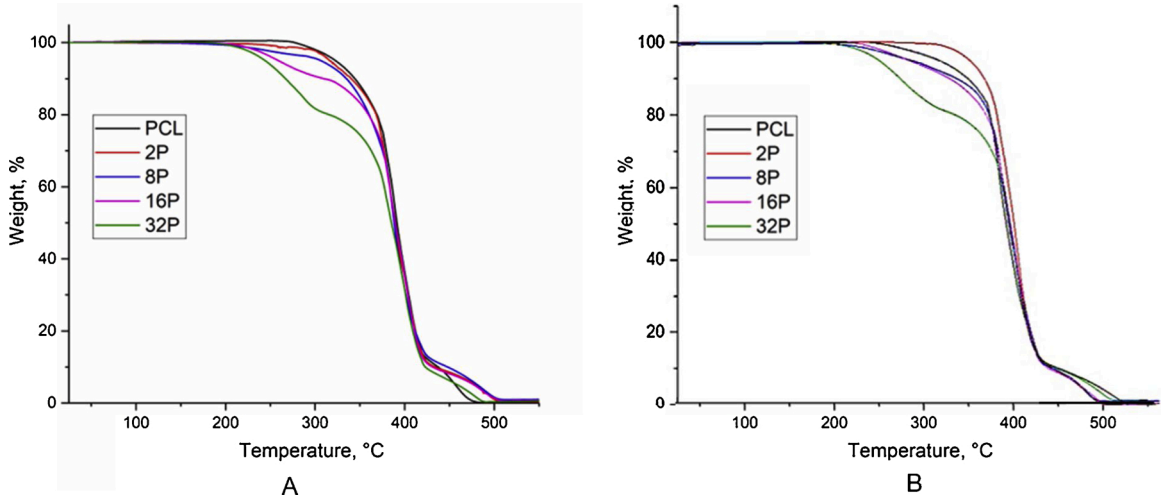

Fig. 5. TGA curves of non-irradiated and irradiated PCL samples with various content of paracetamol: (A) – TGA curves of non-irradiated samples. (B) – TGA curves of irradiated samples.

Table 5
Region of decomposition and T_{max} of scaffolds.

Sample	Before		After	
	Main region of decomposition, °C	T_{max}, °C	Main region of decomposition (°C)	T_{max}, °C
PCL	270–420	391	248–430	398
2 P	220–420	382	280–430	401
8 P	180–420	393	215–430	399
16 P	170–420	255 389	220–430	398
32 P	170–420	278 389	210–430	275 395

exhibits two peaks at 255 °C and 389 °C of T_{max}, while PCL and the composite PCL/paracetamol scaffolds at 385 °C average show only single peak of fast thermal degradation.

E-beam treatment has no critical effect on the thermal properties of materials. However, there is a shift of the thermal decomposition zone towards higher temperatures. This may be attributed to an increase in the degree of crystallinity of the samples [64].

3.5. X-ray diffraction (XRD)

Both molecular weight of the polymer and crystallinity of the material are known to affect the drug release process. Amorphous regions are more likely to release an incorporated drug due to easier diffusion of a drug molecules through looser packed amorphous regions than highly dense crystalline ones [65–67]. It was also reported that drug loading with different drug/polymer ratio can affect polymers crystallinity differently [43,68,69]. Thus, XRD analysis was performed in order to estimate the effect of varying the incorporated drug concentration and further e-beam treatment.

XRD patterns of the PCL and PCL/paracetamol (2, 8, 16 and 32 wt./wt.%) scaffolds are shown in Fig. 6. The pure PCL scaffold pattern contains only the PCL characteristic peaks (2θ = 21° and 24°, corresponding to (110) and (200) crystal planes [70]. With the addition of paracetamol, XRD peaks corresponding to PCL remained at the same angles. Thus, the increasing paracetamol concentration didn't lead to the formation of the new PCL crystalline phases. Paracetamol is known to have three polymorphs: stable form I (monoclinic), metastable form II (orthorhombic), and unstable form III. In this study monoclinic paracetamol (form I) was used. In terms of peak position and peak intensity profile, XRD pattern of the initial drug powder shown in Fig. 5 agree well with one reported in the literature [71,72].

The XRD pattern of the paracetamol loaded scaffolds exhibited the characteristic peaks of both materials, which is more visible on 16 P and 32 P samples due to higher concentration of a drug component. There are no extra peaks and/or peak shift in the XRD patterns of scaffolds since no chemical reaction occurs between the spinning solution components.

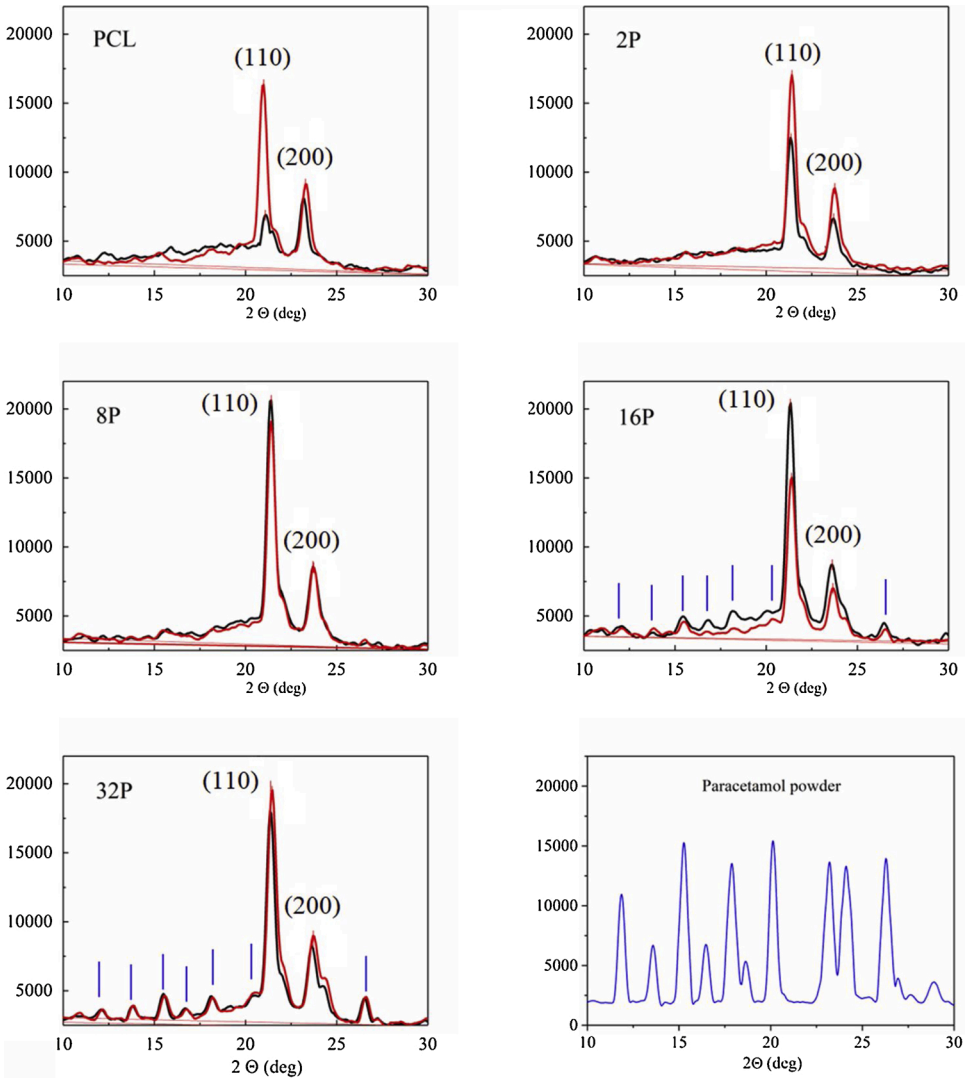

Fig. 6. XRD-patterns of PCL scaffolds before e-beam treatment (black line) and after e-beam treatment (red line). PCL – pure PCL, 2 P, 8 P, 16 P, 32 P – paracetamol loaded fibers with 2, 8, 16, 32 wt./wt.% loading, respectively. XRD-pattern of pure paracetamol powder obtained from the supplier is depicted with a blue line. Blue strokes on 16 P and 32 P samples' patterns show peaks corresponded to paracetamol (For interpretation of the references to colour in this figure legend, the reader is referred to the web version of this article.).

The increased intensity of PCL peaks in paracetamol loaded samples indicates increase in the degree of scaffold crystallinity (Fig. 7). Moreover, the dependence of the degree of scaffold crystallinity on the loaded drug concentration is not linear: 8 P sample demonstrated the highest value and 16 P has less crystalline regions than both 8 P and 32 P samples. This might be due to some interactions among the molecules of PCL and paracetamol during solvent evaporation process. It is known that drug-polymer interactions in matrix drug delivery systems is highly sensitive to drug content: with increase of the initial drug concentration drug state could change from molecular dispersion to solid crystals formation and also the diffusion and migration of drugs can occur during the drying process resulting in an uneven drug distribution across the fiber [12,73]. Paracetamol is highly soluble in alcohols [74], in particular, in hexafluoroisopropanol (HFIP) used in this study as the electrospinning solvent, so drug molecules have sufficient potential for migration with the solvent to the fiber surface during its evaporation and scaffold formation. Crystalline peaks of paracetamol could be observed on 16 P and 32 P samples diffractograms (Fig. 6) meaning that a part of the drug content is presented in crystalline state. This also correlates with TGA analysis (Fig. 5) showing that thermal decomposition of samples with high dug loading (16 P and 32 P) contains paracetamol decomposition stage.

The degree of scaffold crystallinity also increases after e-beam treatment (Fig. 7) but the effect is less prominent with the rise of paracetamol concentration. These changes could be attributed to the reorientation of the shorter chains of polymer as crystallization of the polymer depends on ability of its molecules to align themselves to form regularly ordered regions. Shorter macromolecules chains with fewer chain entanglements can easily undergo this process. Thus, the decrease in molecular weight could lead to the increase in polymer crystallinity.

Average crystallite size was also calculated (Table 6).

Results show that crystallite size values in all samples are similar, which demonstrates that polymer crystallization is associated with the increase in crystallites' number and not with their growth.

3.6. Wettability

One of the crucial properties of scaffolds is the wettability of the surface. It is important not only for successful integration with the body, but also for the release of drugs [15]. The faster the scaffold surface is wetted and subsequently swollen, the faster and more complete the release occurs [11]. Therefore, in order to evaluate the effect of drug concentration and e-beam treatment on scaffolds wettability, we measured the contact angle and calculated the surface energy (Fig. 8).

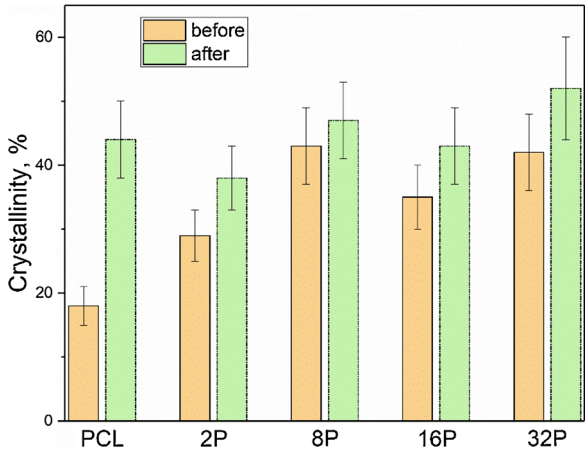

Fig. 7. Degree of polymer crystallinity in non-irradiated (orange bins) and irradiated (green bins) PCL scaffolds (For interpretation of the references to colour in this figure legend, the reader is referred to the web version of this article.).

Table 6
Average crystalline size in the bulk of non-irradiated and irradiated PCL scaffolds.

	Crystalline size, nm				
Sample	PCL	2 P	8 P	16 P	32 P
Before e-beam treatment	13.6 ± 3.26	17.0 ± 1.0	17.5 ± 0.3	13.6 ± 3.3	12.4 ± 3.9
After e-beam treatment	16.2 ± 1.2	16.1 ± 0.5	16.0 ± 0.9	15.2 ± 2.0	13.6 ± 2.8

An increase in drug concentration up to 32 % does not affect wettability. All samples remained hydrophobic, which is typical for synthetic polymers. The treatment does not affect the wettability due to the low absorbed dose [33,75]. However, sample 32 P showed increase in hydrophilicity. This may be because of the increased surface roughness related to the presence of crystals on the surface of the fibers, as shown by SEM [76].

Overall values of surface energy increase with increasing drug concentration. Moreover, the samples are dominated by the dispersion component, which is expected, since PCL is hydrophobic, and paracetamol is poorly soluble in water [77].

3.7. Drug release

The release of drugs from fibers is a complex process that includes several parallel processes: desorption, diffusion, and degradation of the polymer base. Here we present the first hour of the experiment only because release curves corresponding to all samples reached plateau by the end of this period. Results of full 24 h experiment is attached in supplementary information section (Fig. 3, Supplementary). During 24 h of immersion in PBS, paracetamol release is mainly wetting, swelling and desorption controlled, because PCL hydrolytic degradation in aquatic environments and in vivo is a long process which can take from several month to years depending on test product parameters [78,79].

Paracetamol release curves from monolayer materials are shown in Fig. 9.

Firstly, we evaluated how an increase in the concentration of a drug in a spinning solution affects its release from scaffolds. The suggested TTP and QTP values determined for each kinetic curve are presented in Table 7.

All samples perform burst release of paracetamol. Moreover, this is can be most clearly observed in the 2 P sample with the minimal TTP. Drug release rate, its characteristics such as QTP and TTP and presence of burst release effect depend also on drug state (molecular dispersion, particles, crystals etc.) and distribution across the fiber [12]. In addition, the drug dissolves and releases faster from amorphous regions of the polymer. In general, samples with a higher drug load release more drug in one time period as expected. QTP for 16 P samples is higher than for 2 P despite the higher crystallinity of fiber due to the fact that there is 8 times difference in drug loading so in 16 P samples more surface segregated drug molecules are in the direct contact with release medium. The maximum QTP is observed in the 16 P sample. The sample with 32 P, despite the high load, releases slightly less drug, which may be due to the significant crystallinity of the fiber (Fig. 6), considering the difference in loading being only twice as high as for 16 P sample, so the effect of "direct contact", observed during the comparison of 2 P and 16 P, is less prominent. Moreover, it is known that a drug in crystalline state dissolves slower than in an amorphous state [80]. There are visible crystals on the surface of 32 P samples, the amount of drug in crystalline state is higher in 32 P samples than in 16 P samples according to XRD and TGA data. Low QTP for 8 P can be explained by highest crystallinity of polymer matrix.

Electron beam processing of single layer materials increases QTP, but

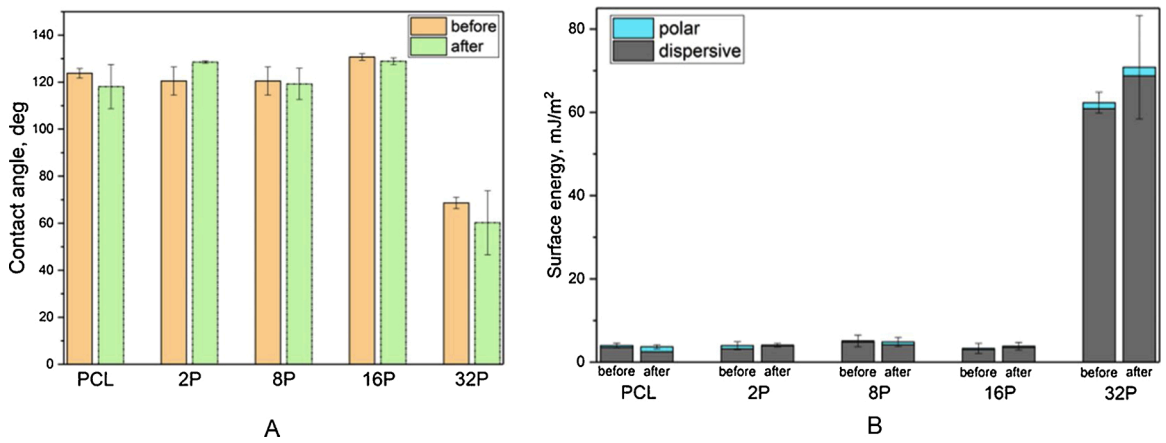

Fig. 8. Water contact angle (A) of pure PCL and paracetamol-loaded non-irradiated (orange bind) and irradiated (green bins) PCL scaffolds. Surface energy of PCL scaffolds: polar part (blue) and dispersive part (grey) (For interpretation of the references to colour in this figure legend, the reader is referred to the web version of this article.).

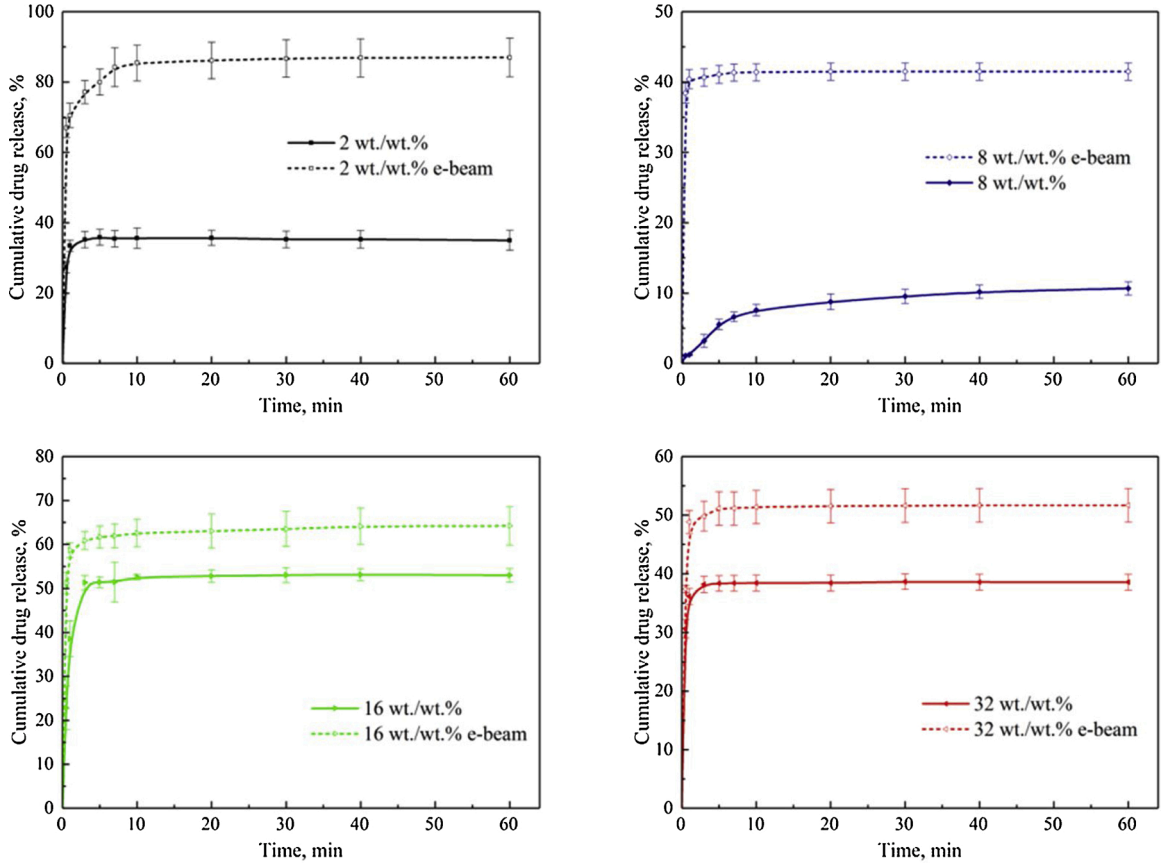

Fig. 9. Paracetamol release kinetics profile from monolayer electrospun PCL scaffolds before (solid lines) and after (dashed lines) e-beam treatment.

Table 7
Time to plateau and quantity to plateau corresponding to paracetamol release from monolayer electrospun PCL scaffolds before and after e-beam treatment.

Sample	2 P		8 P		16 P		32 P	
	Before	After	Before	After	Before	After	Before	After
TTP, min	3	10	20	3	5	2	5	5
QTP, %	35.0 ± 2.8	87.0 ± 5.5	10.7 ± 0.9	41.5 ± 1.2	53.0 ± 1.6	64.2 ± 4.4	38.6 ± 1.4	64.2 ± 4.4

does not significantly affect TTP. This may be due to a decrease in the molecular weight of the polymer and facilitation of drug diffusion due to the removal of internal stresses in the crystalline regions due to a short-term thermal exposure. We presented similar tendencies in our previous work observing ibuprofen release from monolayer PCL scaffolds [81].

Further we evaluated the contribution of the barrier to the drug release process. Paracetamol release curves from composite materials are shown in Fig. 10.

As expected, the addition of barrier layers decreases QTP and simultaneously increases TTP for all groups of samples (Table 8). This is due to the presence of a diffusion barrier, which prevents the inner layers of the material from wetting with water and hinders the transport of drug molecules into the buffer medium.

The simultaneous use of barrier layers and electron beam irradiation can lead to both an increase in TTP and an increase in QTP. In other words, the release is steadier and more complete without the burst release effect. Moreover, this approach is most effective for the middle of the chosen drug to polymer ratio range – 8 and 16 wt./wt.%. The maximum effect is observed for 16 P samples due to high initial crystallinity of 8 P samples fiber. 2 P samples have less drug incorporated and therefore less surface segregated drug so the average diffusion path for drug molecules is longer resulting in lower QTP during the experiment time period.

3.8. Mechanical testing

Despite the confirmed efficiency of applying the e-beam treatment to control the drug release, it is important to assess what effect irradiation has on the mechanical properties of the obtained materials. Accurate measurement of mechanical properties of electrospun scaffolds for biomedical applications is essential to guarantee they can withstand the forces during surgical operation and those exerted by physiological activities and/or by tissue growth [82].

Results of tensile properties testing are presented in a Fig. 11.

Adding the paracetamol powder to the spinning solution results in mechanical properties differences between groups of samples. Compared with pure PCL scaffolds, elongation at break and tensile strength values are lower in drug-loaded samples. Moreover, both values decrease with the increase in paracetamol concentration. Young's modulus increases with paracetamol loading up to 16 wt./wt.% and decreases after further increase in drug concentration. This behavior could be attributed to the differences in fiber compounds' properties because fiber diameters and their distributions do not differ. Visible paracetamol crystals on the 32 P fibers' surface can lead to the assumption of the crystal's presence in the bulk of the material. Hard crystals and/or thinning a polymer parts of a fiber cross-section may lead to the loss in scaffold elasticity.

Composite three-layer materials show similar mechanical behavior in stress-strain tests due to the fact that most material body consists of pure PCL fibers. Elongation at break and tensile strength fluctuate around one value with a slight decrease for C32 PC samples, what correlates with the initial 32 P scaffold's properties. Elongation at break value of composite scaffolds is higher than corresponding one-layer drug-loaded materials and is the same as for pure PCL samples except C32 PC because of the reason stated above. Tensile strength and Young's modulus of composites is lower than pure PCL, moreover Young's modulus decreases ~2.8× (times) comparing to corresponding composites and one-layer scaffolds. C32 PC and 32 P samples demonstrate no difference due to initial low elasticity of 32 P scaffolds.

E-beam treatment affects mechanical properties of all groups of the materials obtained. While having no impact on elongation at break scaffolds, it reduces both their tensile strength and Young's modulus. Because irradiation is not associated with reduction in fiber diameter, molecular weight decrease observed in this study and crystallinity

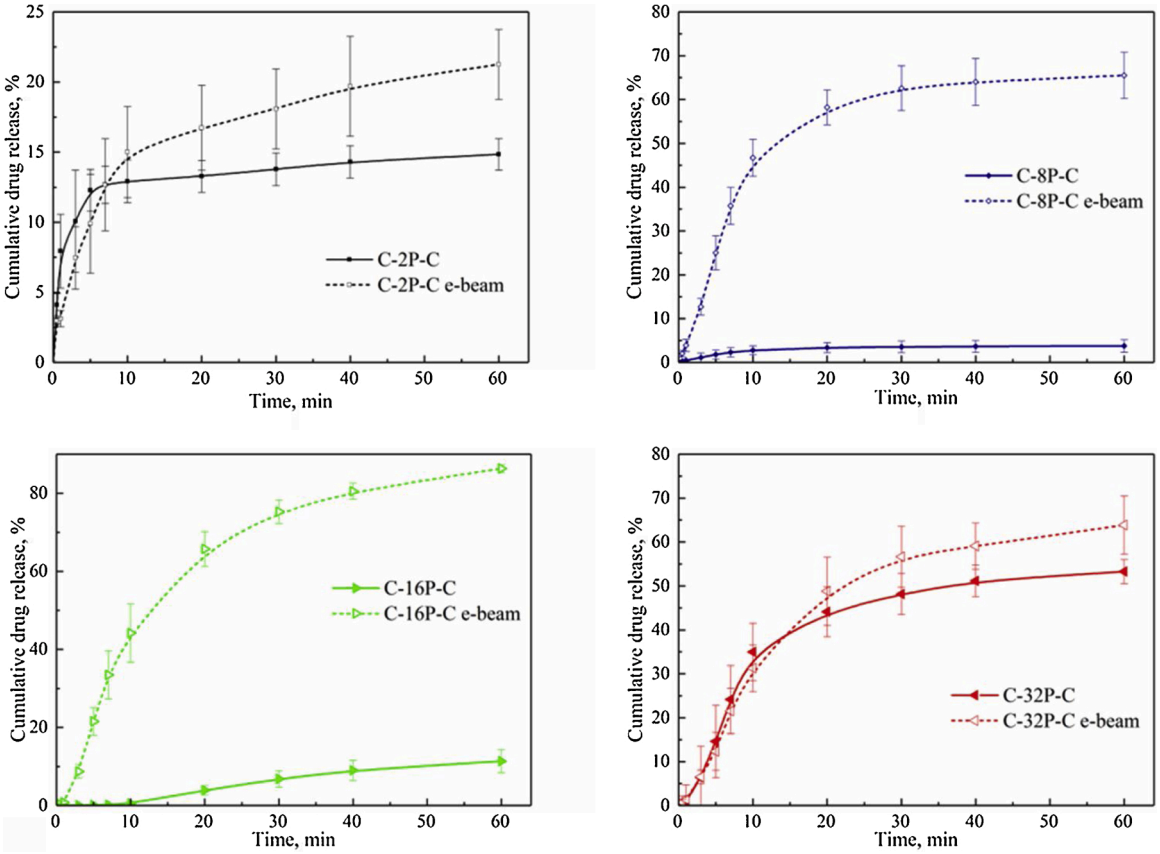

Fig. 10. Paracetamol release kinetics profile from composite electrospun PCL scaffolds before (solid lines) and after (dashed lines) e-beam treatment.

Table 8
Time to plateau and quantity to plateau corresponding to paracetamol release from composite electrospun PCL scaffolds before and after e-beam treatment.

Sample	C2 PC		C8 PC		C16 PC		C32 PC	
	Before	After	Before	After	Before	After	Before	After
TTP, min	20	60	30	30	40	40	30	30
QTP, %	14,8 ± 1,1	21,3 ± 2,5	3,8 ± 1,4	65,5 ± 5,3	11,4 ± 2,9	86,3 ± 1,0	53,3 ± 2,7	63 ± 6,6

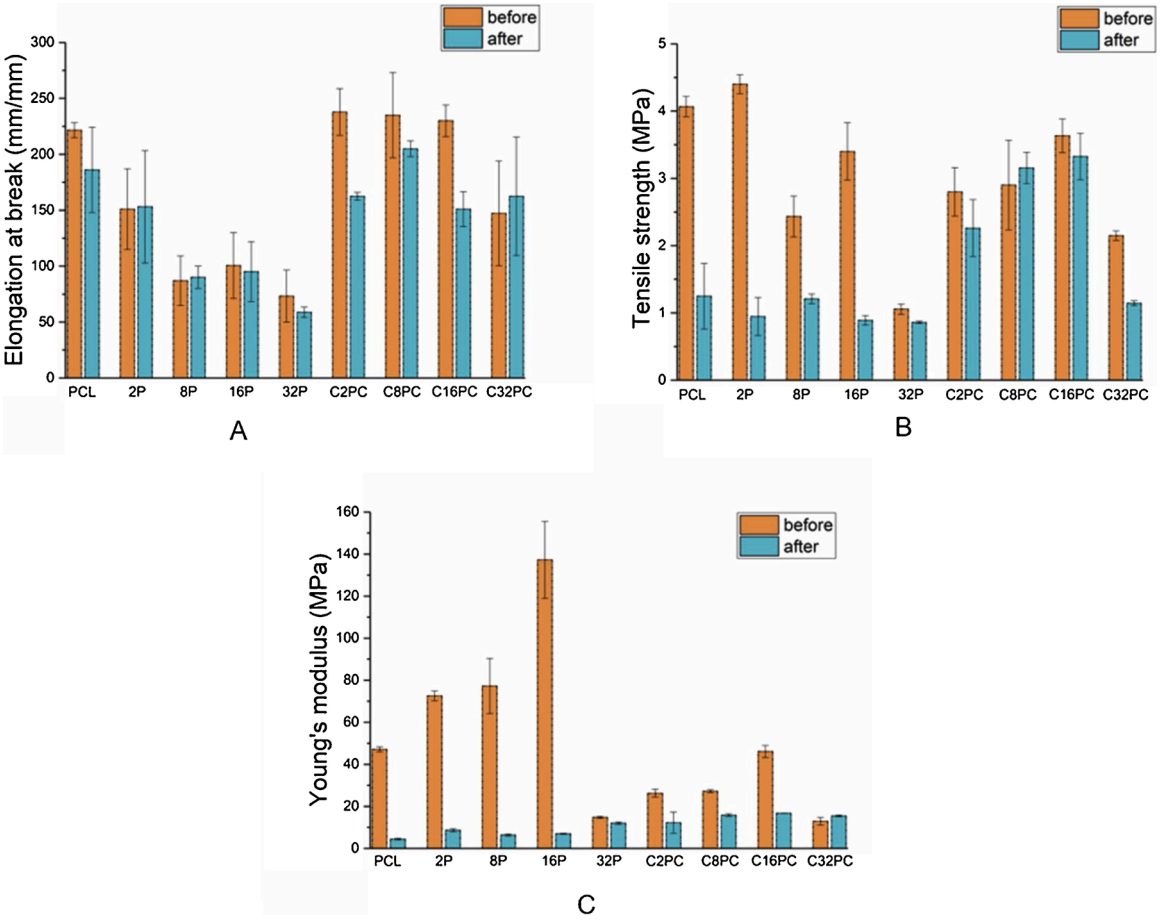

Fig. 11. Tensile testing results for electrospun PCL scaffolds before e-beam treatment (orange bins) and after e-beam treatment (teal bins). Elongation at break (A), Tensile strength (B) and Young's modulus (C) were calculated from stress strain curves for n = 5 samples of each.

changes could be a possible reason. Pure PCL scaffold loses 4× (times) in ultimate tensile strength and 10× (times) in Young's modulus but changes in composites' characteristics are less prominent what can be explained by 3×(times) thicker scaffolds for e-beam to penetrate.

Crystallinity is one of the main contributors for the changes in mechanical properties of polymers. In our work after e-beam treatment of PCL the crystallinity slightly increase when due to the crosslinking of the amorphous phase of the PCL (Fig. 6). The amorphous phase plays role of the load bearing elements in the material by connecting the crystalline domains. Thus the scission of the polymer chains in the amorphous phase leaves the crystalline domains untied leading to the decrease of mechanical properties of the polymer as was previously reported in [20].

Though e-beam irradiation has obvious negative effect on scaffolds' mechanical properties this effect is not crucial to further medical application as elongation at break of a weakest sample (32 P after irradiation) is around 300 %, average value for irradiated one-layer materials varies from around 800 % to 300 % and from around 1000 % to 750 % for irradiated composites [70].

4. Conclusions

We have obtained monolayer and composite scaffolds based on polycaprolactone/paracetamol and processed them with a pulsed electron beam.

It has been shown that barrier layers increase TTP, e-beam irradiation increases QTP, and the combination of these methods is effective for completing a steady drug release without the burst release effect. The main reason for the observed effects is a decrease in polymer molecular weight due to electron beam irradiation and the creation of a diffusion barrier slowing down swelling and diffusion.

At the same time, the thermal and mechanical properties of materials do not deteriorate significantly and remain sufficient for its application. The obtained patterns and the developed approach can be useful for creating effective targeted delivery and controlled release devices for radiation-resistant drugs. Such devises can be used in reconstructive and anticancer therapy, osteogenesis and transplantation, to prevent the development of surgical infections and other applications associated with delivery of poorly water-soluble radiation-resistant drugs, including cytostatics and antibiotics.

The proposed parameters of TTP (time to plateau) and QTP (quantity to plateau) can be useful for researchers to describe and compare the results of studying the kinetic curves of the active substances release from carrier devices.

Funding

This research was financially supported by Tomsk Polytechnic University within the assignment of the Ministry of Science and Higher Education of the Russian Federation.

CRediT authorship contribution statement

Apollinariya A. Volokhova: Methodology, Investigation, Visualization, Writing - original draft. **Valeriya L. Kudryavtseva:** Methodology, Writing - original draft. **Tatiana I. Spiridonova:** Data curation. **Ilya Kolesnik:** Investigation. **Semen I. Goreninskii:** Investigation. **Roman V. Sazonov:** Methodology, Investigation. **Gennady E. Remnev:** Methodology, Resources. **Sergei I. Tverdokhlebov:** Conceptualization, Supervision, Project administration, Funding acquisition, Writing - review & editing.

Declaration of Competing Interest

The authors report no declarations of interest.

Acknowledgements

We thank Mr. D. Novikov, head of Laboratory of physical-chemical analytical methods of Tomsk State University, for providing Gel-penetration chromatography facilities and "Materials Science Shared Center", part of the Tomsk Regional Common Use Center (TRCUC) for providing XRD and mechanical testing equipment.

Appendix A. Supplementary data

Supplementary material related to this article can be found, in the online version, at doi:https://doi.org/10.1016/j.mtcomm.2021.102134.

References

[1] S. Thakkar, M. Misra, Electrospun polymeric nanofibers: new horizons in drug delivery, Eur. J. Pharm. Sci. 107 (2017) 148–167, https://doi.org/10.1016/j.ejps.2017.07.001.
[2] J. Siepmann, R.A. Siegel, M.J. Rathbone, Fundamentals and Applications of Controlled Release Drug Delivery, Springer US, Boston, MA, 2012, https://doi.org/10.1007/978-1-4614-0881-9.
[3] Y. Zykova, V. Kudryavtseva, M. Gai, A. Kozelskaya, J. Frueh, G. Sukhorukov, S. Tverdokhlebov, Free-standing microchamber arrays as a biodegradable drug depot system for implant coatings, Eur. Polym. J. 114 (2019) 72–80, https://doi.org/10.1016/j.eurpolymj.2019.02.029.
[4] A.V. Ermakov, V.L. Kudryavtseva, P.A. Demina, R.A. Verkhovskii, J. Zhang, E. V. Lengert, A.V. Sapelkin, I.Y. Goryacheva, G.B. Sukhorukov, Site-specific release of reactive oxygen species from ordered arrays of microchambers based on polylactic acid and carbon nanodots, J. Mater. Chem. B (2020), https://doi.org/10.1039/D0TB01148G.
[5] E. Rompen, O. Domken, M. Degidi, A.E. Farias Pontes, A. Piattelli, The effect of material characteristics, of surface topography and of implant components and connections on soft tissue integration: a literature review, Clin. Oral Implants Res. 17 (2006) 55–67.
[6] S.R. Taylor, D.F. Gibbons, Effect of surface texture on the soft tissue response to polymer implants, J. Biomed. Mater. Res. 17 (1983) 205–227, https://doi.org/10.1002/jbm.820170202.
[7] B. Dhandayuthapani, Y. Yoshida, T. Maekawa, D.S. Kumar, Polymeric scaffolds in tissue engineering application: a review, Int. J. Polym. Sci. 2011 (2011) 1–19, https://doi.org/10.1155/2011/290602.
[8] S.-F. Chou, D. Carson, K.A. Woodrow, Current strategies for sustaining drug release from electrospun nanofibers, J. Control. Release 220 (2015) 584–591, https://doi.org/10.1016/j.jconrel.2015.09.008.
[9] V. Kudryavtseva, K. Stankevich, A. Kozelskaya, E. Kibler, Y. Zhukov, A. Malashicheva, A. Golovkin, A. Mishanin, V. Filimonov, E. Bolbasov, S. Tverdokhlebov, Magnetron plasma mediated immobilization of hyaluronic acid for the development of functional double-sided biodegradable vascular graft, Appl. Surf. Sci. 529 (2020), 147196, https://doi.org/10.1016/j.apsusc.2020.147196.
[10] J.M. Cornejo Bravo, L.J. Villarreal Gómez, A. Serrano Medina, Electrospinning for drug delivery systems: drug incorporation techniques. Electrospinning - Mater. Tech. Biomed. Appl., InTech, 2016, https://doi.org/10.5772/65939.
[11] D.-G. Yu, J.-J. Li, G.R. Williams, M. Zhao, Electrospun amorphous solid dispersions of poorly water-soluble drugs: a review, J. Control. Release 292 (2018) 91–110, https://doi.org/10.1016/j.jconrel.2018.08.016.
[12] X. Huang, C.S. Brazel, On the importance and mechanisms of burst release in matrix-controlled drug delivery systems, J. Control. Release 73 (2001) 121–136, https://doi.org/10.1016/S0168-3659(01)00248-6.
[13] O. Cars, W.A. Craig, Pharmacodynamics of antibiotics-consequences for dosing: proceedings of a symposium held in Stockholm, June 7–9, 1990, Scand. J. Infect. Dis. 22 (1990) 1–284, https://doi.org/10.3109/inf.1990.22.suppl-74.01.
[14] J.M. Klaase, B.B.R. Kroon, C. Benckhuijsen, A.N. van Geel, C.E. Albus-Lutter, J. Wieberdink, Results of regional isolation perfusion with cytostatics in patients with soft tissue tumors of the extremities, Cancer 64 (1989) 616–621, https://doi.org/10.1002/1097-0142(19890801)64:3<616::AID-CNCR2820640309>3.0.CO;2-8.
[15] M.V. Natu, H.C. de Sousa, M.H. Gil, Electrospun Drug-Eluting Fibers for Biomedical Applications, 2011, pp. 57–85, https://doi.org/10.1007/8415_2010_56.
[16] T. Okuda, K. Tominaga, S. Kidoaki, Time-programmed dual release formulation by multilayered drug-loaded nanofiber meshes, J. Control. Release 143 (2010) 258–264, https://doi.org/10.1016/j.jconrel.2009.12.029.
[17] S. Kidoaki, I.K. Kwon, T. Matsuda, Mesoscopic spatial designs of nano- and microfiber meshes for tissue-engineering matrix and scaffold based on newly devised multilayering and mixing electrospinning techniques, Biomaterials (2005), https://doi.org/10.1016/j.biomaterials.2004.01.063.
[18] D.G. Petlin, S.I. Tverdokhlebov, Y.G. Anissimov, Plasma treatment as an efficient tool for controlled drug release from polymeric materials: a review, J. Control. Release 266 (2017) 57–74, https://doi.org/10.1016/j.jconrel.2017.09.023.
[19] V. Kudryavtseva, K. Stankevich, E. Kibler, A. Golovkin, A. Mishanin, E. Bolbasov, E. Choynzonov, S. Tverdokhlebov, The deposition of thin titanium-nitrogen coatings on the surface of PCL-based scaffolds for vascular tissue engineering, Appl. Phys. Lett. (2018), https://doi.org/10.1063/1.5017580.
[20] R. Navarro, G. Burillo, E. Adem, A. Marcos-Fernández, Effect of ionizing radiation on the chemical structure and the physical properties of polycaprolactones of different molecular weight, Polymers (Basel) 10 (2018) 397, https://doi.org/10.3390/polym10040397.
[21] R. Malinowski, Some effects of radiation treatment of biodegradable PCL/PLA blends, J. Polym. Eng. 38 (2018) 635–640, https://doi.org/10.1515/polyeng-2017-0311.
[22] A.A. El-Saftawy, A. Elfalaky, M.S. Ragheb, S.G. Zakhary, Electron beam induced surface modifications of PET film, Radiat. Phys. Chem. 102 (2014) 96–102, https://doi.org/10.1016/j.radphyschem.2014.04.025.
[23] M.-L. Cairns, A. Sykes, G.R. Dickson, J.F. Orr, D. Farrar, A. Dumba, F.J. Buchanan, Through-thickness control of polymer bioresorption via electron beam irradiation, Acta Biomater. 7 (2011) 548–557, https://doi.org/10.1016/j.actbio.2010.09.012.
[24] S.C.J. Loo, H.T. Tan, C.P. Ooi, Y.C.F. Boey, Hydrolytic degradation of electron beam irradiated high molecular weight and non-irradiated moderate molecular weight PLLA, Acta Biomater. 2 (2006) 287–296, https://doi.org/10.1016/j.actbio.2005.10.003.
[25] X. Zhang, M. Kotaki, S. Okubayashi, S. Sukigara, Effect of electron beam irradiation on the structure and properties of electrospun PLLA and PLLA/PDLA blend nanofibers, Acta Biomater. 6 (2010) 123–129, https://doi.org/10.1016/j.actbio.2009.06.007.
[26] V.L. Kudryavtseva, E.N. Bolbasov, D.V. Ponomarev, G.E. Remnev, S. I. Tverdokhlebov, The influence of pulsed Electron beam treatment on properties of PLLA nonwoven materials produced by solution blow spinning, Bionanoscience (2017), https://doi.org/10.1007/s12668-017-0436-9.
[27] M. Simpson, B.F. Gilmore, A. Miller, J. Helt-Hansen, F.J. Buchanan, Irradiation of bioresorbable biomaterials for controlled surface degradation, Radiat. Phys. Chem. (2014), https://doi.org/10.1016/j.radphyschem.2013.09.002.
[28] S. Burkert, T. Schmidt, U. Gohs, H. Dorschner, K.-F. Arndt, Cross-linking of poly(N-vinyl pyrrolidone) films by electron beam irradiation, Radiat. Phys. Chem. 76 (2007) 1324–1328, https://doi.org/10.1016/j.radphyschem.2007.02.024.
[29] R.L. Clough, S.W. Shalaby, Radiation Effects on Polymers, American Chemical Society, 1991.
[30] A.-S. Crucq, V. Deridder, B. Tilquin, Radiostability of pharmaceuticals under different irradiation conditions, Radiat. Phys. Chem. 72 (2005) 355–361, https://doi.org/10.1016/j.radphyschem.2004.02.006.
[31] L. Varshney, P.B. Dodke, Radiation effect studies on anticancer drugs, cyclophosphamide and doxorubicin for radiation sterilization, Radiat. Phys. Chem. 71 (2004) 1103–1111, https://doi.org/10.1016/j.radphyschem.2003.12.052.
[32] B.K. Singh, D.V. Parwate, I.B. Dassarma, S.K. Shukla, Radiation sterilization of fluoroquinolones in solid state: investigation of effect of gamma radiation and electron beam, Appl. Radiat. Isot. 68 (2010) 1627–1635, https://doi.org/10.1016/j.apradiso.2010.04.002.
[33] G. Abuhanoğlu, A.Y. Ozer, Radiation effects on pharmaceuticals, Fabad J. Pharm. Sci. 35 (2010) 203–217.
[34] D. Mondal, M. Griffith, S.S. Venkatraman, Polycaprolactone-based biomaterials for tissue engineering and drug delivery: current scenario and challenges, Int. J. Polym. Mater. Polym. Biomater. 65 (2016) 255–265, https://doi.org/10.1080/00914037.2015.1103241.

[35] H. Kweon, A novel degradable polycaprolactone networks for tissue engineering, Biomaterials 24 (2003) 801–808, https://doi.org/10.1016/S0142-9612(02)00370-8.

[36] O.S. Manoukian, M.R. Arul, N. Sardashti, T. Stedman, R. James, S. Rudraiah, S. G. Kumbar, Biodegradable polymeric injectable implants for long-term delivery of contraceptive drugs, J. Appl. Polym. Sci. 135 (2018), 46068, https://doi.org/10.1002/app.46068.

[37] L.E. Visscher, H.P. Dang, M.A. Knackstedt, D.W. Hutmacher, P.A. Tran, 3D printed Polycaprolactone scaffolds with dual macro-microporosity for applications in local delivery of antibiotics, Mater. Sci. Eng. C 87 (2018) 78–89, https://doi.org/10.1016/j.msec.2018.02.008.

[38] G. Buschle-Diller, J. Cooper, Z. Xie, Y. Wu, J. Waldrup, X. Ren, Release of antibiotics from electrospun bicomponent fibers, Cellulose 14 (2007) 553–562, https://doi.org/10.1007/s10570-007-9183-3.

[39] J.G. Merrell, S.W. McLaughlin, L. Tie, C.T. Laurencin, A.F. Chen, L.S. Nair, Curcumin-loaded poly(ε-caprolactone) nanofibres: diabetic wound dressing with anti-oxidant and anti-inflammatory properties, Clin. Exp. Pharmacol. Physiol. 36 (2009) 1149–1156, https://doi.org/10.1111/j.1440-1681.2009.05216.x.

[40] S.E. Kim, Y.-P. Yun, Y.-K. Han, D.-W. Lee, J.-Y. Ohe, B.-S. Lee, H.-R. Song, K. Park, B.-J. Choi, Osteogenesis induction of periodontal ligament cells onto bone morphogenic protein-2 immobilized PCL fibers, Carbohydr. Polym. 99 (2014) 700–709, https://doi.org/10.1016/j.carbpol.2013.08.053.

[41] K.S. Stankevich, I.A. Schepetkin, S.I. Goreninskii, A.K. Lavrinenko, E.N. Bolbasov, A.R. Kovrizhina, L.N. Kirpotina, V.D. Filimonov, A.I. Khlebnikov, S. I. Tverdokhlebov, M.T. Quinn, Poly(ε-caprolactone) scaffolds doped with c-Jun N-terminal kinase inhibitors modulate phagocyte activation, ACS Biomater. Sci. Eng. (2019), https://doi.org/10.1021/acsbiomaterials.9b01401.

[42] S. Goreninskii, E. Bolbasov, E.A. Sudarev, K. Stankevich, Y. Anissimov, A. Golovkin, A.I. Mishanin, A. Viknianshchuk, V. Filimonov, S. Tverdokhlebov, Fabrication and Properties of L-arginine-doped PCL Electrospun Composite Scaffolds, 2017, https://doi.org/10.1016/j.matlet.2017.11.115.

[43] T. Potrč, S. Baumgartner, R. Roškar, O. Planinšek, Z. Lavrič, J. Kristl, P. Kocbek, Electrospun polycaprolactone nanofibers as a potential oromucosal delivery system for poorly water-soluble drugs, Eur. J. Pharm. Sci. 75 (2015) 101–113, https://doi.org/10.1016/j.ejps.2015.04.004.

[44] A. Fahr, X. Liu, Drug delivery strategies for poorly water-soluble drugs, Expert Opin. Drug Deliv. (2007), https://doi.org/10.1517/17425247.4.4.403.

[45] I. Egorov, V. Esipov, G. Remnev, M. Kaikanov, E. Lukonin, A. Poloskov, A high-repetition rate pulsed electron accelerator, IEEE Trans. Dielectr. Electr. Insul. (2013), https://doi.org/10.1109/TDEI.2013.6571453.

[46] V.L. Kudryavtseva, E.N. Bolbasov, D.V. Ponomarev, G.E. Remnev, S. I. Tverdokhlebov, The influence of pulsed electron beam treatment on properties of PLLA nonwoven materials produced by solution blow spinning, Bionanoscience (2018), https://doi.org/10.1007/s12668-017-0436-9.

[47] X. Wang, H. Zhao, L.S. Turng, Q. Li, Crystalline morphology of electrospun poly (ε-caprolactone) (PCL) nanofibers, Ind. Eng. Chem. Res. (2013), https://doi.org/10.1021/ie302185e.

[48] T. Walles, T. Herden, A. Haverich, H. Mertsching, Influence of scaffold thickness and scaffold composition on bioartificial graft survival, Biomaterials 24 (2003) 1233–1239, https://doi.org/10.1016/S0142-9612(02)00490-8.

[49] W. Cui, X. Li, X. Zhu, G. Yu, S. Zhou, J. Weng, Investigation of drug release and matrix degradation of electrospun poly(dl-lactide) fibers with paracetanol inoculation, Biomacromolecules 7 (2006) 1623–1629, https://doi.org/10.1021/bm060057z.

[50] M. Chen, P.K. Patra, S.B. Warner, S. Bhowmick, Role of fiber diameter in adhesion and proliferation of NIH 3T3 fibroblast on electrospun polycaprolactone scaffolds, Tissue Eng. (2007), https://doi.org/10.1089/ten.2006.0205.

[51] S. Seif, L. Franzen, M. Windbergs, Overcoming drug crystallization in electrospun fibers – elucidating key parameters and developing strategies for drug delivery, Int. J. Pharm. 478 (2015) 390–397, https://doi.org/10.1016/j.ijpharm.2014.11.045.

[52] J. Xie, C.-H. Wang, Electrospun micro- and nanofibers for sustained delivery of paclitaxel to treat C6 glioma in vitro, Pharm. Res. 23 (2006) 1817–1826, https://doi.org/10.1007/s11095-006-9036-z.

[53] R.A. Thakur, C.A. Florek, J. Kohn, B.B. Michniak, Electrospun nanofibrous polymeric scaffold with targeted drug release profiles for potential application as wound dressing, Int. J. Pharm. 364 (2008) 87–93, https://doi.org/10.1016/j.ijpharm.2008.07.033.

[54] E.B. Burgina, V.P. Baltakhinov, E.V. Boldyreva, T.P. Shakhtschneider, IR spectra of paracetamol and phenacetin. 1. Theoretical and experimental studies, J. Struct. Chem. 45 (2004) 64–73, https://doi.org/10.1023/B:JORY.0000041502.85584.d5.

[55] O. Persenaire, M. Alexandre, P. Degée, P. Dubois, Mechanisms and kinetics of thermal degradation of poly(ε-caprolactone), Biomacromolecules 2 (2001) 288–294, https://doi.org/10.1021/bm0056310.

[56] S.C.J. Loo, C.P. Ooi, Y.C.F. Boey, Radiation effects on poly(lactide-co-glycolide) (PLGA) and poly(l-lactide) (PLLA), Polym. Degrad. Stab. 83 (2004) 259–265, https://doi.org/10.1016/S0141-3910(03)00271-4.

[57] G.E. Kholodnaya, R.V. Sazonov, D.V. Ponomarev, G.E. Remnev, A.V. Poloskov, Pulsed electron beam propagation in gases under pressure of 6.6 kPa in drift tube, Nucl. Instrum. Methods Phys. Res. Sect. B Beam Interact. Mater. Atoms. (2017), https://doi.org/10.1016/j.nimb.2016.12.010.

[58] R. Malinowski, Effect of electron radiation and triallyl isocyanurate on the average molecular weight and crosslinking of poly(ε-caprolactone), Polym. Adv. Technol. (2016), https://doi.org/10.1002/pat.3610.

[59] C. Ramkissoon-Ganorkar, F. Liu, M. Baudyš, S.W. Kim, Modulating insulin-release profile from pH/thermosensitive polymeric beads through polymer molecular weight, J. Control. Release 59 (1999) 287–298, https://doi.org/10.1016/S0168-3659(99)00006-1.

[60] G. Mittal, D.K. Sahana, V. Bhardwaj, M.N.V. Ravi Kumar, Estradiol loaded PLGA nanoparticles for oral administration: effect of polymer molecular weight and copolymer composition on release behavior in vitro and in vivo, J. Control. Release 119 (2007) 77–85, https://doi.org/10.1016/j.jconrel.2007.01.016.

[61] Y. Li, H. Pang, Z. Guo, L. Lin, Y. Dong, G. Li, M. Lu, C. Wu, Interactions between drugs and polymers influencing hot melt extrusion, J. Pharm. Pharmacol. 66 (2014) 148–166, https://doi.org/10.1111/jphp.12183.

[62] Y. Wan, X. Lu, S. Dalai, J. Zhang, Thermophysical properties of polycaprolactone/chitosan blend membranes, Thermochim. Acta 487 (2009) 33–38, https://doi.org/10.1016/j.tca.2009.01.007.

[63] W.A. Herrera-Kao, M.I. Loría-Bastarrachea, Y. Pérez-Padilla, J.V. Cauich-Rodríguez, H. Vázquez-Torres, J.M. Cervantes-Uc, Thermal degradation of poly (caprolactone), poly(lactic acid), and poly(hydroxybutyrate) studied by TGA/FTIR and other analytical techniques, Polym. Bull. 75 (2018) 4191–4205, https://doi.org/10.1007/s00289-017-2260-3.

[64] F.C. Bragança, D.S. Rosa, Thermal, mechanical and morphological analysis of poly (ε-caprolactone), cellulose acetate and their blends, Polym. Adv. Technol. (2003), https://doi.org/10.1002/pat.381.

[65] M. Miyajima, A. Koshika, J. Okada, M. Ikeda, K. Nishimura, Effect of polymer crystallinity on papaverine release from poly (l-lactic acid) matrix, J. Control. Release 49 (1997) 207–215, https://doi.org/10.1016/S0168-3659(97)00081-3.

[66] J.-C. Jeong, J. Lee, K. Cho, Effects of crystalline microstructure on drug release behavior of poly(ε-caprolactone) microspheres, J. Control. Release 92 (2003) 249–258, https://doi.org/10.1016/S0168-3659(03)00367-5.

[67] E. Luong-Van, L. Grøndahl, K.N. Chua, K.W. Leong, V. Nurcombe, S.M. Cool, Controlled release of heparin from poly(ε-caprolactone) electrospun fibers, Biomaterials 27 (2006) 2042–2050, https://doi.org/10.1016/j.biomaterials.2005.10.028.

[68] L.J. del Valle, R. Camps, A. Díaz, L. Franco, A. Rodríguez-Galán, J. Puiggalí, Electrospinning of polylactide and polycaprolactone mixtures for preparation of materials with tunable drug release properties, J. Polym. Res. 18 (2011) 1903–1917, https://doi.org/10.1007/s10965-011-9597-3.

[69] H. Lian, Z. Meng, Melt electrospinning vs. solution electrospinning: a comparative study of drug-loaded poly (ε-caprolactone) fibres, Mater. Sci. Eng. C 74 (2017) 117–123, https://doi.org/10.1016/j.msec.2017.02.024.

[70] M. Diba, M.H. Fathi, M. Kharaziha, Novel forsterite/polycaprolactone nanocomposite scaffold for tissue engineering applications, Mater. Lett. 65 (2011) 1931–1934, https://doi.org/10.1016/j.matlet.2011.03.047.

[71] G. Nichols, C.S. Frampton, Physicochemical characterization of the orthorhombic polymorph of paracetamol crystallized from solution, J. Pharm. Sci. 87 (1998) 684–693, https://doi.org/10.1021/js970483d.

[72] I.-C. Wang, M.-J. Lee, D.-Y. Seo, H.-E. Lee, Y. Choi, W.-S. Kim, C.-S. Kim, M.-Y. Jeong, G.J. Choi, Polymorph transformation in paracetamol monitored by in-line NIR spectroscopy during a cooling crystallization process, AAPS PharmSciTech 12 (2011) 764–770, https://doi.org/10.1208/s12249-011-9642-x.

[73] K.C. Gupta, A. Haider, Y.R. Choi, I.K. Kang, Nanofibrous scaffolds in biomedical applications, Biomater. Res. (2014), https://doi.org/10.1186/2055-7124-18-5.

[74] R.A. Granberg, Å.C. Rasmuson, Solubility of paracetamol in pure solvents, J. Chem. Eng. Data (1999), https://doi.org/10.1021/je990124v.

[75] X. Zhang, M. Kotaki, S. Okubayashi, S. Sukigara, Effect of electron beam irradiation on the structure and properties of electrospun PLLA and PLLA/PDLA blend nanofibers, Acta Biomater. 6 (2010) 123–129, https://doi.org/10.1016/j.actbio.2009.06.007.

[76] K.J. Kubiak, M.C.T. Wilson, T.G. Mathia, P. Carval, Wettability versus roughness of engineering surfaces, Wear 271 (2011) 523–528, https://doi.org/10.1016/j.wear.2010.03.029.

[77] A. Di Luca, A. Longoni, G. Criscenti, I. Lorenzo-Moldero, M. Klein-Gunnewiek, J. Vancso, C. van Blitterswijk, C. Mota, L. Moroni, Surface energy and stiffness discrete gradients in additive manufactured scaffolds for osteochondral regeneration, Biofabrication 8 (2016), 015014, https://doi.org/10.1088/1758-5090/8/1/015014.

[78] H. Sun, L. Mei, C. Song, X. Cui, P. Wang, The in vivo degradation, absorption and excretion of PCL-based implant, Biomaterials (2006), https://doi.org/10.1016/j.biomaterials.2005.09.019.

[79] B. Lu, G.X. Wang, D. Huang, Z.L. Ren, X.W. Wang, P.L. Wang, Z.C. Zhen, W. Zhang, J.H. Ji, Comparison of PCL degradation in different aquatic environments: effects of bacteria and inorganic salts, Polym. Degrad. Stab. (2018), https://doi.org/10.1016/j.polymdegradstab.2018.02.002.

[80] M. Zamani, M. Morshed, J. Varshosaz, M. Jannesari, Controlled release of metronidazole benzoate from poly ε-caprolactone electrospun nanofibers for periodontal diseases, Eur. J. Pharm. Biopharm. (2010), https://doi.org/10.1016/j.ejpb.2010.02.002.

[81] A.A. Rakina, T.I. Spriridonova, V.L. Kudryavtseva, I.M. Kolesniik, R.V. Sazonov, G. E. Remnev, S.I. Tverdokhlebov, Ibuprofen controlled release from E-beam treated polycaprolactone electrospun scaffolds, J. Phys. Conf. Ser. (2018), https://doi.org/10.1088/1742-6596/1115/3/032051.

[82] A. Cipitria, A. Skelton, T.R. Dargaville, P.D. Dalton, D.W. Hutmacher, Design, fabrication and characterization of PCL electrospun scaffolds—a review, J. Mater. Chem. 21 (2011) 9419, https://doi.org/10.1039/c0jm04502k.